

Role of land cover changes for atmospheric CO₂ increase and climate change during the last 150 years

VICTOR BROVKIN, STEPHEN SITCH, WERNER VON BLOH, MARTIN CLAUSSEN, EVA BAUER and WOLFGANG CRAMER

Potsdam Institute for Climate Impact Research, PO Box 601203, D-14412 Potsdam, Germany

Abstract

We assess the role of changing natural (volcanic, aerosol, insolation) and anthropogenic (CO₂ emissions, land cover) forcings on the global climate system over the last 150 years using an earth system model of intermediate complexity, CLIMBER-2. We apply several datasets of historical land-use reconstructions: the cropland dataset by Ramankutty & Foley (1999) (R&F), the HYDE land cover dataset of Klein Goldewijk (2001), and the land-use emissions data from Houghton & Hackler (2002). Comparison between the simulated and observed temporal evolution of atmospheric CO₂ and $\delta^{13}\text{CO}_2$ are used to evaluate these datasets. To check model uncertainty, CLIMBER-2 was coupled to the more complex Lund–Potsdam–Jena (LPJ) dynamic global vegetation model.

In simulation with R&F dataset, biogeophysical mechanisms due to land cover changes tend to decrease global air temperature by 0.26 °C, while biogeochemical mechanisms act to warm the climate by 0.18 °C. The net effect on climate is negligible on a global scale, but pronounced over the land in the temperate and high northern latitudes where a cooling due to an increase in land surface albedo offsets the warming due to land-use CO₂ emissions.

Land cover changes led to estimated increases in atmospheric CO₂ of between 22 and 43 ppmv. Over the entire period 1800–2000, simulated $\delta^{13}\text{CO}_2$ with HYDE compares most favourably with ice core during 1850–1950 and Cape Grim data, indicating preference of earlier land clearance in HYDE over R&F. In relative terms, land cover forcing corresponds to 25–49% of the observed growth in atmospheric CO₂. This contribution declined from 36–60% during 1850–1960 to 4–35% during 1960–2000. CLIMBER-2-LPJ simulates the land cover contribution to atmospheric CO₂ growth to decrease from 68% during 1900–1960 to 12% in the 1980s. Overall, our simulations show a decline in the relative role of land cover changes for atmospheric CO₂ increase during the last 150 years.

Keywords: atmospheric CO₂ concentration, atmospheric $\delta^{13}\text{CO}_2$, biogeophysical effects, biosphere–atmosphere interaction, earth system modelling, historical land cover changes, interactive carbon cycle

Received 19 June 2003; revised version received 10 December 2003; accepted 23 January 2004

Introduction

Between one-third and one-half of the land surface has been directly transformed by human action (Vitousek *et al.*, 1997). Changes in land cover trigger a chain of feedbacks in the climate system. Deforestation in northern temperate and boreal regions leads to an increase in land surface albedo during snow season and

consequent cooling (e.g. Bonan *et al.*, 1992; Claussen *et al.*, 2001; Ganopolski *et al.*, 2001). This regional cooling, amplified by the sea-ice albedo feedback, propagates to the global scale via atmospheric and oceanic responses. Through changes in transpiration, boreal deforestation affects the partitioning between sensible and latent heat, thereby increasing land surface temperature during summer (Betts, 2001; Brovkin *et al.*, 2003). In tropical regions, large-scale deforestation leads to a reduction in precipitation and an increase in land surface temperature in the deforested region

Correspondence: Victor Brovkin, tel. + 49 331 288 2592, fax + 49 331 288 2570, e-mail: Victor.Brovkin@pik-potsdam.de

(Henderson-Sellers *et al.*, 1993; De Fries *et al.*, 2002). The effects of small-scale tropical deforestation (Avisar *et al.*, 2002), as well as the remote effects of tropical deforestation (Chase *et al.*, 2000), are not clear. Despite complex geographical patterns, the overall effect of historical land cover changes on climate has been estimated as cooling in both equilibrium (Betts, 2001) and transient (Brovkin *et al.*, 1999; Bertrand *et al.*, 2002; Bauer *et al.*, 2003) experiments using climate models.

Most of these studies highlight the biogeophysical effects of land cover change (i.e. changes in albedo, transpiration, and surface roughness) on climate. Associated biogeochemical effects, in particular direct emissions of CO₂ from land conversion, affect atmospheric gas composition, and hence also climate (Fig. 1). Historical cumulative carbon losses due to changes in land use have been estimated to be 180–200 PgC (House *et al.*, 2002). Between 10% and 30% of the current total anthropogenic emissions of CO₂ are caused by land-use conversion (Prentice *et al.*, 2001). Vegetation productivity and soil decomposition respond to changes in atmospheric CO₂ and climate patterns and, thereby, impact terrestrial carbon storage. At the same time, changes in atmospheric CO₂, sea surface temperatures, and oceanic circulation alter patterns of CO₂ solubility and biological productivity and, consequently, oceanic carbon storage. All these mechanisms operate under climatic and CO₂ perturbations induced by climatic variability and changes in natural (e.g. volcanic aerosols, solar irradiation) and anthropogenic (e.g. fossil fuel CO₂) forcing.

The assessment of the effects of land cover changes on the climate system requires a model capable of simulating interactions between all the necessary components of the Earth system, namely the atmosphere, land, ocean, and carbon cycle. Such models can be of different complexity, ranging from one- and two-dimensional models (Wigley & Raper, 1992; Gerber *et al.*, 2003) to full complexity models (Cox *et al.*, 2000; Friedlingstein *et al.*,

2001). To allow long model integrations and maintain broad-scale geographic patterns, we use an Earth system model of intermediate complexity (EMIC), CLIMBER-2 (Petoukhov *et al.*, 2000), and study both biogeophysical and biogeochemical effects of land cover changes on climate. EMICs are simplified but geographically explicit models capable to simulate all the main processes discussed above (Claussen *et al.*, 2002). Computational efficiency of these models allows to perform many sensitivity experiments and to investigate the influence of uncertainty in climatic forcings and process parameterizations on model results (Forest *et al.*, 2002). In the recent IPCC assessment (Prentice *et al.*, 2001), the role of land cover changes in the climate system has been described in terms of CO₂ emissions. Rather than simply estimating the CO₂ emissions, we focus directly on a relative role of land-use change for the increase of atmospheric CO₂ concentration (i.e. the primary climate forcing). We also test the uncertainty due to differences in land cover reconstructions and model parameterizations. Several reconstructions of historical land cover changes during the last 300 years are available at present: (i) cropland dataset of Ramanakutty & Foley (1999) (R&F); (ii) the HYDE land cover dataset (Klein Goldewijk, 2001); and (iii) the land-use emissions dataset of Houghton *et al.* (1982). The latter dataset is based on a land inventory or bookkeeping approach; it has been subsequently improved and transformed into a land-use emission dataset (Houghton & Hackler, 2002) (HGT). The estimates obtained for net land-use flux during the 1980s by the Carbon Cycle Model Linkage Project (CCMLP) based on the R&F dataset are substantially smaller than the fluxes from HGT (McGuire *et al.*, 2001). We investigate the effect of R&F, HYDE, and HGT reconstructions on atmospheric CO₂ within the framework of a climate system model. We test uncertainty in model parameterizations by performing online simulations with a more complex biosphere dynamics model, Lund–Potsdam–Jena (LPJ) (Sitch *et al.*, 2003). Comparison between the simulated and observed temporal evolution of atmospheric CO₂ and δ¹³C are used to evaluate model runs.

Methods

CLIMBER-2 is a climate system model of intermediate complexity (Petoukhov *et al.*, 2000). It includes a 2.5-dimensional dynamical–statistical atmosphere model with a coarse spatial resolution of 10° latitude and 51° longitude, a multibasin, zonally averaged ocean model, a sea-ice model with latitudinal resolution of 2.5° and a terrestrial vegetation model. Results from CLIMBER-2 compare favourably with data of the present-day climate, paleoclimatic reconstructions (Claussen *et al.*,

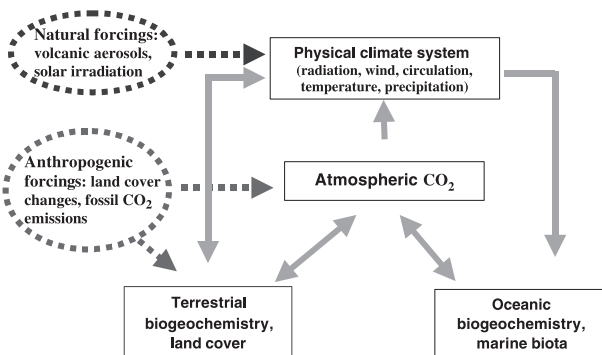


Fig. 1 External forcings and feedbacks in the climate system accounted for in the model simulations.

1999), and with results from sensitivity experiments undertaken with comprehensive models (Ganopolski *et al.*, 2001). The model has been recently upgraded incorporating a model for oceanic biogeochemistry including a marine biota model and tested for the Holocene period (Brovkin *et al.*, 2002). In the following simulations, the parameters of CLIMBER-2 are kept the same as in the preindustrial simulation AOV-0K discussed by Brovkin *et al.* (2002).

In all simulations, atmosphere, ocean, and vegetation components are interactive, accounting for both physical and chemical feedbacks. In particular, atmospheric CO₂ is interactive and resolved on an annual time step:

$$C_A(t+1) = C_A(t) + \beta(E(t) + F_{OA}(t) + F_{LA}(t)), \quad (1)$$

where C_A is the atmospheric CO₂ concentration (ppmv), E is the fossil fuel emission (PgC yr⁻¹), F_{OA} and F_{LA} are annual ocean-atmosphere and land-atmosphere carbon fluxes (PgC yr⁻¹), respectively, and β is the conversion factor. As a first approximation, biogeochemical processes with time scales greater than millennia (oceanic sedimentation, weathering, peat accumulation, and mineralization) are ignored.

Forcings

Two types of external forcings have been applied in the simulations: natural and anthropogenic. For the natural forcings, we employed a reconstruction of solar irradiance and volcanic forcing by Crowley (2000), both normalized to 1365 W m⁻². For further details see descriptions of forcings S_{14} and V in Bauer *et al.* (2003). Trend in solar irradiance is important to match the observed increase in temperature during the first half of 20th century. Radiative forcing due to sulphate aerosols and non-CO₂ greenhouse gases were neglected in the simulations; in a first approximation, these forcings are similar in amplitude but different in sign on the global scale. Solar and volcanic forcings shown in Fig. 2a are used in all simulations.

Anthropogenic forcing includes fossil fuel CO₂ emissions and historical land cover changes. The former for years 1750–1999 are taken from Marland *et al.* (2002) (MBA data) (Fig. 2c). Before 1750, emissions are neglected. Emission forcing is the only anthropogenic forcing in simulation E. Forcing due to historical land cover changes is explained hereafter and denoted with an H in the simulation acronym (see Table 1). For historical land cover changes we employ the R&F dataset for the years 1700–1992, except in simulations EH-HYDE and EH-HGT. Timing of land cover changes prior to 1700 is highly uncertain; for simplicity, a linear interpolation of data is used for years 1000–1700.

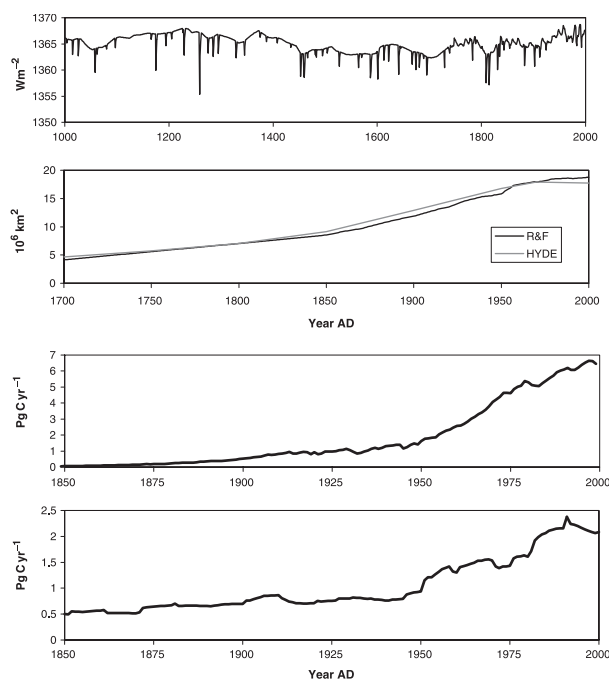


Fig. 2 Forcings applied in the simulations. (a) Changes in solar irradiance and volcanic forcing (Bauer *et al.*, 2003); (b) decrease in globally averaged tree area in accordance with R&F and HYDE land cover datasets; (c) fossil fuel emissions from MBA; (d) land-use emission from HGT.

Between 1992 and 2000, we linearly extrapolate the R&F dataset using the trend between the 1980s and the 1970s decadal averages. The data were aggregated to the coarse spatial resolution of CLIMBER-2.

In CLIMBER-2, vegetation cover is described in terms of fractions of trees and grasses, while the R&F dataset specifies land cover changes in terms of crop fraction. We interpret changes in cropland area as changes in tree area, although, in general, deforestation and increase in crop fraction are not the same. For example, the latter might be due to conversion of grassland. Nevertheless, the historical increase in crop area is approximately equal to the decrease in forest area. Unlike R&F, HYDE explicitly resolves changes in forested area. We assume crop ecosystems function in a way similar to grasslands.

In all simulations, initial conditions at the year 1000 AD are taken as the prehistorical equilibrium simulated for present-day orbital forcing, constant insolation of 1365 W m⁻², absence of volcanic eruptions and land cover changes, and atmospheric $p\text{CO}_2 = 280$ ppmv. Each grid cell is divided into natural and cropland fractions. Vegetation in the natural fraction evolves freely in response to climate change. If the tree fraction is reduced, then a carbon flux associated with removal of tree biomass is emitted directly into atmosphere. This

Table 1 List of simulation experiments done for the study

Simulation	Fossil fuel CO ₂ emissions	Reconstruction of land cover change	Terrestrial carbon flux
CONTROL	–	–	CLIMBER
E*	MBA [†]	–	CLIMBER
H*	–	R&F [‡]	CLIMBER
H_P [‡]	–	R&F	–
H_C [‡]	–	R&F	CLIMBER
EH (baseline)	MBA	R&F	CLIMBER
EH-HYDE	MBA	HYDE [†]	CLIMBER
EH-HGT	MBA	HGT [†] (CO ₂ flux), R&F (biophysics)	HGT + CLIMBER
E-LPJ	MBA	–	LPJ, years 1900–1992
EH-LPJ	MBA	R&F	LPJ, years 1900–1992

*E in the simulation acronym is for CO₂ emissions, H for historical land cover changes.

[†]MBA is for data by Marland *et al.* (2002), R&F for Ramankutty and Foley (1999), HYDE for Klein Goldewijk (2001), HGT for Houghton & Hackler (2002).

[‡]H_P, biogeophysical effects only; H_C, biogeochemical effects only.

is simplified in comparison with approaches by Houghton *et al.* (1982), McGuire *et al.* (2001), and Leemans *et al.* (2002), where dynamics of forestry and agricultural products in pools with different time scales are accounted for. As a consequence, CLIMBER-2 simulations might slightly overestimate CO₂ flux associated with land cover change (this is different in the CLIMBER-LPJ simulations discussed below). Abandoned crop area is available for regrowth of natural vegetation. In all simulations, changes in tree cover affected climate via changes in land surface biophysics and atmospheric CO₂.

Uncertainty in land cover data

Data and models are subject to uncertainty. We used the HYDE dataset to test the effect of a different land cover dataset on atmospheric CO₂ dynamics. HYDE specifies changes in forest (woodland) area explicitly while its temporal resolution, 50 years during 1700–1950 and 20 years during 1950–1990, is coarser than the annual resolution of R&F dataset. We used a version of HYDE with natural vegetation cover simulated by BIOME1. HYDE has discrete classes of vegetation on a spatial resolution of 0.5° × 0.5°; during upscaling to coarse CLIMBER-2 resolution the data were transformed to fraction of deforested area. For the periods 1000–1700 and 1990–2000 we applied the same data interpolation as for the R&F dataset.

Besides R&F and HYDE datasets, we used HGT dataset of land-use emissions. The dataset for years 1850–2000 includes only emissions due to land conversion to agriculture. Changes in terrestrial carbon storage due to climate and CO₂ change are not included. In the simulation EH-HGT, we use land cover changes from R&F dataset until 1850, and HGT

land cover change CO₂ emissions thereafter. Changes in land carbon storage due to climate and CO₂ change are simulated by CLIMBER-2.

Uncertainty in model parameterizations

To address uncertainty in parameterizations of the vegetation model, we coupled CLIMBER-2 with LPJ-DGVM (Sitch *et al.*, 2003), which includes more mechanisms and is typically used at a higher spatial resolution than the VECODE vegetation model used in CLIMBER-2. This allows LPJ to resolve the seasonal dynamics of biogeochemical processes, including a coupled plant production–water balance scheme, resource competition, population dynamics, and fire disturbance (Thonicke, *et al.*, 2001). Vegetation is represented by a larger set of 10 plant functional types (PFTs) differentiated by physiological, morphological, phenological, bioclimatic, and fire-response attributes.

In our coupled simulations, LPJ is used with a spatial resolution of 0.5° latitude/longitude and is called at the end of the every CLIMBER-2 simulation year. CLIMBER-2 provides LPJ with monthly anomalies of surface air temperature, precipitation, and cloudiness, which are added to the background climate patterns from the CRU climate dataset of the Climate Research Unit, University of East Anglia (New *et al.*, 1999, 2000). Absolute anomalies are used for temperature and cloudiness and relative anomalies for precipitation.

Monthly land–atmosphere carbon fluxes simulated by LPJ are summed over the year and over every grid cell. This annual global sum, $F_{LA}(t)$ is passed onto CLIMBER-2 and used to calculate atmospheric CO₂ concentration for the next year, see Eqn (1). The simulated atmospheric CO₂ is used as input for LPJ in calculating $F_{LA}(t)$ in the next year, thus creating a

biogeochemical feedback between LPJ and CLIMBER-2. Biogeophysical feedback of land cover changes on climate is simulated by VECODE.

As LPJ simulates fire disturbance, it needs inter-annually variable climate in order to correctly simulate global vegetation. CLIMBER-2 simulates the long-term (decadal to millennia) trend in climate, but not interannual climate variability. To account for the latter in the coupled simulations, we used a cyclic replication of CRU monthly climatology for years 1901–1930 during the 1000 years spinup. The model has been initialized with land cover for the year 1901 after running for a spinup using pre-1900 atmospheric CO₂ and climate patterns simulated by CLIMBER-2 from the EH simulation.

For each transient year (1901–1992), a year between 1901 and 1930 was randomly selected. The corresponding set of 12 months CRU climatology is updated with climate anomalies from CLIMBER-2 and used to drive LPJ. To yield statistically significant results, we repeated coupled simulations 40 times and calculated mean average and standard deviation of the simulation ensemble. In simulation EH-LPJ, the R&F dataset was used as the land cover forcing after the year 1901. Land carbon fluxes were calculated in accordance with the approach by McGuire *et al.* (2001).

Results

Effect of land cover changes on global temperature

Climate change in simulation H is a product of two effects, biogeophysical (changes in albedo, transpiration) and biogeochemical (changes in atmospheric CO₂

concentration). To separate these effects, we performed two additional sensitivity simulations, H_P and H_C. In simulation H_P, the radiative effect of CO₂ released to the atmosphere due to land cover changes is ignored (i.e. biogeophysical effect only). Changes in mean annual global temperature relative to the CONTROL simulation are presented in Fig. 3. In simulation H_P, temperature decreases by 0.26 °C in year 2000. Before 1850, changes in temperature are rather small (–0.1 °C), and they accelerate after 1850 (Fig. 3). Temperature dynamics approximately follow the trend in deforested area (Fig. 2b). The cooling, due to biogeophysical forcing, is in line with results from other studies using General Circulation models (GCMs), (Betts, 2001) and EMICs (Bertrand *et al.*, 2002; Matthews *et al.*, 2003).

In simulation H_C, the radiative effect of CO₂ emitted to the atmosphere due to land cover changes is accounted for while biophysical effects are neglected (i.e. biogeochemical effect only). Due to growth in atmospheric CO₂ concentration, the climate becomes warmer, with temperature increases of 0.18 °C by year 2000.

In simulation H, biogeochemically induced warming opposes biogeophysical cooling. The global mean annual temperature shows a slightly decreasing trend, with a decrease of 0.05 °C by 2000 relative to the CONTROL (Fig. 3). This temperature decrease occurs despite an increase of 18 ppmv in atmospheric CO₂ in simulation H. This small net change, albeit within the natural variability of the climate system, is clearly detectable with the statistical–dynamical atmospheric module of CLIMBER-2, which averages synoptic-scale variability and allows quantification of the effect of small radiative forcings (Petoukhov *et al.*, 2000).

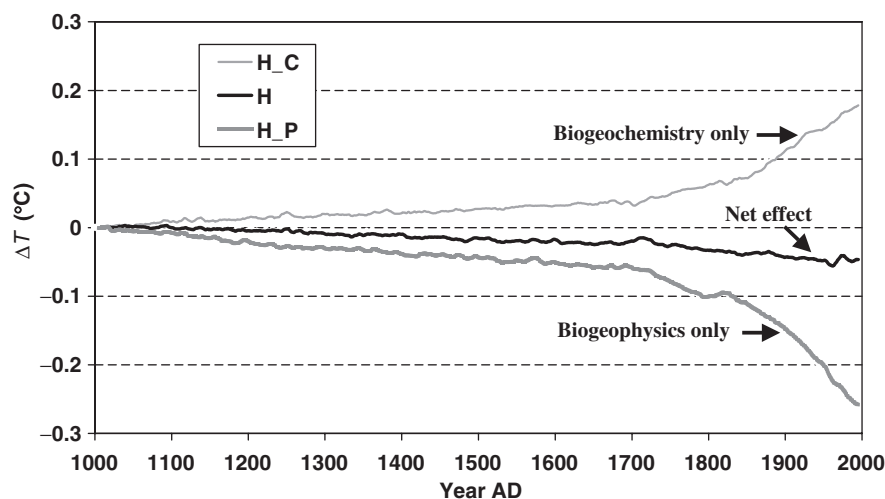


Fig. 3 Effect of historical land cover changes on global mean annual temperature: H_P, biogeophysical effect only; H_C, biogeochemical effect only; H, both biogeophysical and biogeochemical effects. A 10-year moving average of anomalies relative to the CONTROL simulation is shown.

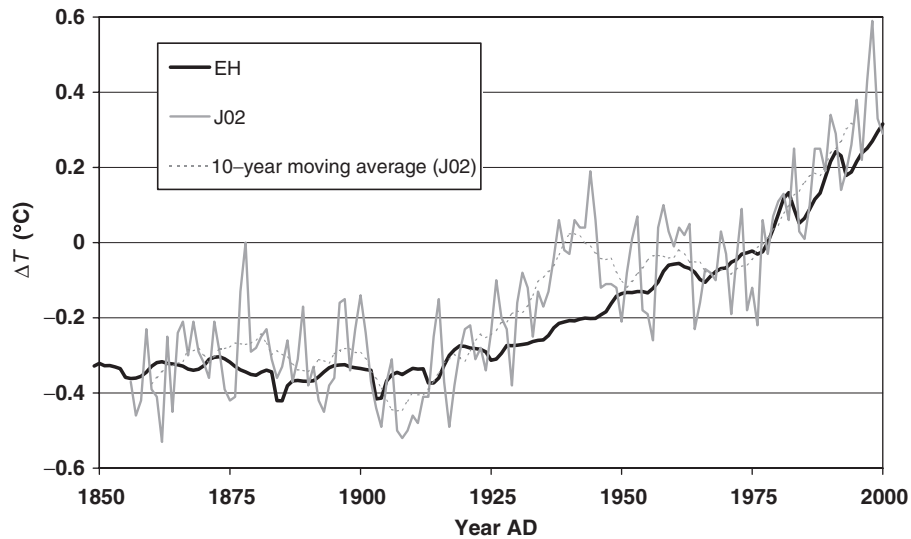


Fig. 4 Simulated global annual temperature anomalies normalized to 1961–1990. Grey solid line – observation data by Jones *et al.* (2001); grey dashed line – 10-year moving average for data by Jones *et al.* (2001); black solid line – EH simulation.

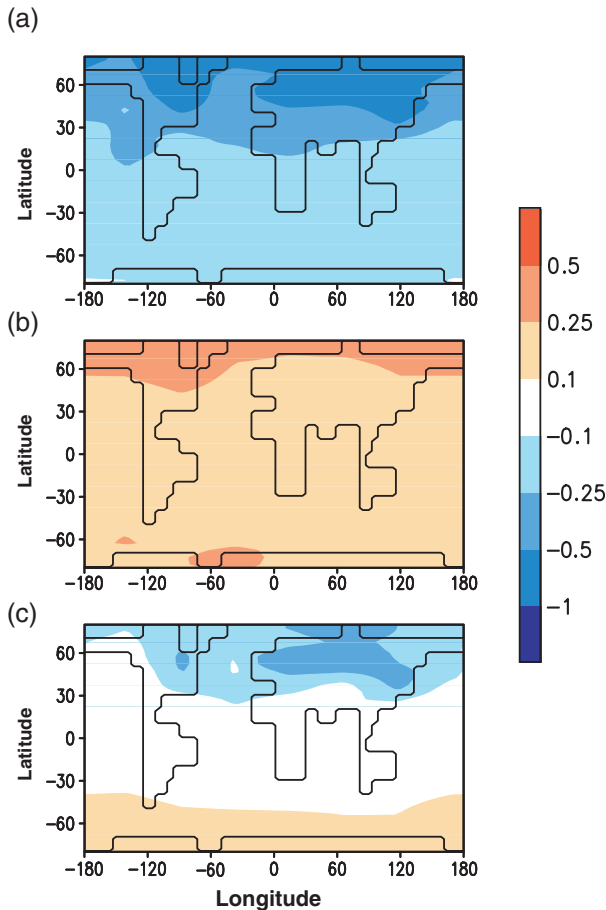


Fig. 5 Simulated changes in mean annual temperatures (°C). (a) H_P simulation; (b) H_C simulation, (c) H simulation. Changes during the 1990s relative to the CONTROL simulation are shown.

Altogether, the forcings produce an increase in temperature similar to that observed over the last 150 years (Fig. 4). During the second part of the 19th century, the temperature stays nearly constant despite increases in atmospheric CO₂. Here, the effect of increasing atmospheric CO₂ on temperature is counterbalanced by the biogeophysical effect of deforestation. Therefore, deforestation forcing might be necessary to explain and reproduce changes in temperature during the second half of the 19th century. In the 20th century, the main trend is an increase of temperature due to increasing atmospheric CO₂ and solar irradiance. For a detailed discussion of the effects of these forcings on the climate of the last millennium using CLIMBER-2, see Bauer *et al.* (2003).

Regional climate changes

Geographical distribution of annual temperature changes is shown in Fig. 5. In simulation H_P, all regions show a decrease in temperature with the largest change of over -0.5°C in the land regions in the temperate and high northern latitudes (Fig. 5a). This is because the forcing originates in these regions and propagates to the global scale mainly through changes in sea surface temperatures and sea-ice cover. In contrast to the biogeophysical forcing, CO₂ forcing is not region specific but global due to the fast atmospheric mixing of emitted CO₂. Increased CO₂ concentration leads to a global warming, which is more pronounced in the polar regions due to the sea-ice albedo feedback (Fig. 5b). The net effect of both forcings is negligible over the tropical regions but quite

significant over the extratropical regions in the Northern hemisphere, especially over Eurasia (Fig. 5c). Over the regions covered in winter by snow, the biogeophysical cooling dominates over the biogeochemical warming.

Response of atmospheric CO₂ to the forcings

According to the Law Dome data (Etheridge *et al.*, 1996), atmospheric CO₂ fluctuated around the pre-industrial concentration of 280 ppmv until the 19th century. By year 2000, atmospheric CO₂ reached a concentration of 369 ppmv at Mauna Loa (Keeling & Whorf, 2002). Assuming Mauna Loa is representative of the whole globe, growth in atmospheric CO₂ during the last millennium was 89 ppmv. To separate the effect of land cover changes in this CO₂ growth from the role of fossil fuel emissions, we performed simulation E with emissions only, simulations H with historical land cover changes only following R&F dataset, and simulation EH with both forcings (see Fig. 6 and Table 1).

Years 1850–1940. In the Law Dome data, this period is characterized by a cumulative CO₂ growth of 25 ppmv, with an almost constant rate of 0.3 ppmv yr⁻¹ between 1875 and 1940. Increases in atmospheric CO₂ during this period are 10, 7, and 18 ppmv in the E, H, and EH simulations, respectively (Table 2). While cumulative emissions from MBA data are 47 PgC, or 22 ppmv in terms of atmospheric CO₂ concentration, the ocean absorbs about one-half of this amount and only 10 ppmv is left in the atmosphere in the E simulation. Land cover changes lead to an 8 ppmv growth of atmospheric CO₂ (difference between the EH and H simulations). Observed CO₂ growth during 1850–1940

is 7 ppmv higher than in the EH simulation. Possible reasons for the too slow CO₂ growth in the model might be an underestimation of deforestation during this period as well as the impact of natural climate variability on the carbon cycle, which is unaccounted for in the simulations.

Years 1940–1950. The period between 1938 and 1950 is interesting because of an almost constant atmospheric CO₂ recorded at Law Dome, despite substantial fossil fuel emissions (about 1.3 PgC yr⁻¹). In the E simulation, CO₂ growth during the 1940s was 2.6 ppmv. The EH simulation revealed an additional CO₂ increase of 0.7 ppmv due to land cover changes (Table 2), as the R&F dataset shows slowing rate of deforestation during this decade. Since the period includes the Second World War, land-use statistics for this period may not be very reliable. Nevertheless, even without any land-use changes (E simulation), atmospheric CO₂ grows at a rate comparable to previous decades. We conclude that the stalling of atmospheric CO₂ during the 1940s was unlikely to have been caused by changes in land cover, although this might be one of the contributing factors. Other factors, like internal variability of the climate system, may also be responsible (Joos *et al.*, 1999). Better statistics for land cover changes during the 1940s would help to clarify the role of land cover changes in this period.

Years 1950–2000. Rapid CO₂ growth during the second half of the 20th century from 311 to 369 ppmv is mostly caused by the accelerated growth of fossil fuel emissions. The E simulation reveals a 52 ppmv increase due to fossil fuel emission. EH simulates an

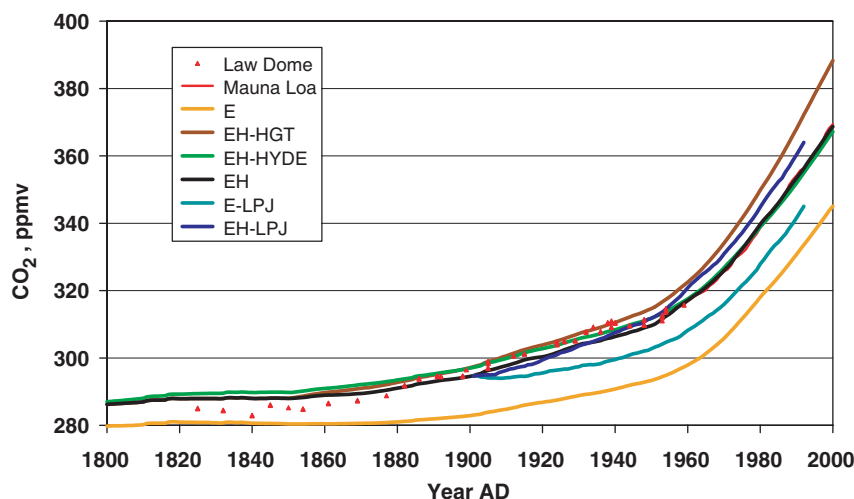


Fig. 6 Atmospheric CO₂ concentration from the CLIMBER-2 and CLIMBER2-LPJ simulations during years 1800–2000 against Law Dome ice core data (Etheridge *et al.*, 1996) and Mauna Loa observations (Keeling & Whorf, 2002).

Table 2 Increase in the atmospheric CO₂ (ppmv), simulations against observations

Simulation/observations	Years 1000–2000	Years 1000–1850	Years 1850–1940	Years 1940–1950	Years 1950–2000
Law Dome/Mauna Loa*	89	5	25	0 ± 1	58
E	65	0	10	2.6	52
H	18	8	7	0.2	3
EH (baseline)	89	8	18	3.3	59
EH-HYDE	87	10	19	3.4	55
EH-HGT	108	8	23	4.1	74
E-LPJ	65(76) [†]	8	12	3.2	42(45)
EH-LPJ	84(76)	8	20	4.2	52(45)

*Data by Etheridge *et al.* (1996) and Keeling & Whorf (2002).

[†]The values for LPJ simulations are for years 1900–1992 only; numbers in parentheses are for observed data during the same period as for LPJ.

E in the simulation acronym is for CO₂ emissions, H for historical land cover changes, HYDE is for data by Klein Goldewijk (2001), HGT for Houghton & Hackler (2002); LPJ, Lund–Potsdam–Jena.

increase of 59 ppmv, or an additional growth of 7 ppmv due to land cover changes. While this value is almost the same as that during period 1850–1950 (9 ppmv), the relative role of land cover changes in atmospheric CO₂ growth between 1950 and 2000 is substantially lower due to growth of CO₂ emissions. At the end of the 20th century, the terrestrial biosphere becomes a carbon sink in the model, mostly due to effect of elevated CO₂ concentration on plant productivity. In the EH simulation, land was a sink of 1.0 and 1.4 Pg C yr⁻¹ during the 1980s and the 1990s, respectively. Oceanic uptake was 1.5 and 1.7 Pg C yr⁻¹ for the same periods (Table 3). These estimates are within the range given in recent studies (Prentice *et al.*, 2001; Bopp *et al.*, 2002; Plattner *et al.*, 2002) (see Table 3). In the model, oceanic and land uptake during the 1980s is 2.5 Pg C yr⁻¹. This is larger than the observed value of 2.1 Pg C yr⁻¹ (Table 3), indicating simulated land uptake of 1.0 Pg C yr⁻¹ is too high. Nonetheless, accounting for coarse model resolution and simplified assumptions about vegetation processes, the model simulates the trend in atmospheric CO₂ during 1950–2000 surprisingly well (Fig. 6). Over the entire period 1000–1999, cumulative fossil fuel emissions are 277 Pg C from MBA, with simulated (EH) oceanic uptake of 121 Pg C, and land source of 33 Pg C. These values are very close to estimates of 280, 124, and 34 Pg C for emissions, oceanic uptake, and net land source, respectively, from House *et al.* (2002).

Simulations with HYDE, HGT datasets

In the EH-HYDE simulation, atmospheric CO₂ dynamics is quite similar to the CO₂ trend in the EH simulation (Fig. 6). Until 1950, CO₂ concentration in the EH-HYDE is higher than in EH by up to 3 ppmv because of higher deforestation in the early period. Between 1880

and 1950, EH-HYDE is in better agreement with CO₂ observations than EH, presumably due to an earlier deforestation in the HYDE data. Simulated atmospheric CO₂ follows observations closely between 1950 and 1970. During the 1970s and the 1980s, simulated atmospheric CO₂ growth is slower than observed as well as that simulated with the R&F dataset. This is mainly due to rather high terrestrial uptake (1.3 Pg C yr⁻¹). During the 1990s, extrapolation of the 1970–1990 trends from HYDE dataset until 2000 worked surprisingly well, resulting in terrestrial and oceanic uptake of 1.5 and 1.6 Pg C yr⁻¹, respectively, in line with the IPCC estimates (Prentice *et al.*, 2001). In year 2000, simulated CO₂ was 2 ppmv lower than observed (and the EH simulation). In comparison with R&F data, HYDE data indicates a slightly reduced role of land cover changes in atmospheric CO₂ growth, or 22 ppmv (a difference between the EH-HYDE and E simulations).

The EH-HGT simulation starts to deviate from the EH after 1850. Until 1940, simulated atmospheric CO₂ follows Law Dome data with an increase of 23 ppmv between 1850 and 1940. During the 1940s, CO₂ grows by 4.1 ppmv, slightly higher than 3.3 and 3.4 ppmv simulated in the EH and EH-HYDE runs, respectively. During the second half of the 20th century, CO₂ growth is 74 ppmv, 16 ppmv higher than observed. This growth is explained by a high release of CO₂ from the land in HGT data. For example, the average land-use flux in HGT dataset is 2.0 and 2.2 Pg C yr⁻¹ during the 1980s and the 1990s, respectively. Simulated carbon uptake due to CO₂ growth and climate change is 1.8 and 2.2 Pg C yr⁻¹ for the 1980s and the 1990s, respectively. As a result, the land is a net source of 0.2 Pg C yr⁻¹ during the 1980s and neutral during the 1990s, while ocean uptake is 1.7 and 2.0 Pg C yr⁻¹ during these periods (Table 3).

Table 3 Simulated carbon fluxes* during 1980–1999 (PgC yr⁻¹) and comparison with the other estimates

Simulation	Years 1980–1989		Years 1990–1999 [†]	
	Land	Ocean	Land	Ocean
E	-1.5	-1.3	-1.8	-1.5
H	0.2	-0.2	0.1	-0.2
EH (baseline)	-1.0	-1.5	-1.4	-1.7
EH-HYDE	-1.3	-1.4	-1.5	-1.6
EH-HGT	0.2	-1.7	0	-2.0
E-LPJ	-1.2	-1.3		
EH-LPJ	-0.5	-1.6		
Other estimates				
Prentice <i>et al.</i> (2001)	-0.2 ± 0.7	-1.9 ± 0.6	-1.4 ± 0.7	-1.7 ± 0.5
Plattner <i>et al.</i> (2002)	-0.4 ± 0.7	-1.7 ± 0.6	-0.7 ± 0.8	-2.4 ± 0.7
Bopp <i>et al.</i> (2002)	-0.3 ± 0.9	-1.8 ± 0.8	-1.2 ± 0.9	-2.3 ± 0.7

*In accordance with the IPCC approach (Prentice *et al.*, 2001), negative flux values mean uptake of carbon by land (ocean), while positive value corresponds to release of land (ocean) carbon to atmosphere.

[†]Values from Bopp *et al.* (2002) averaged over the period 1990–1996.

E in the simulation acronym is for CO₂ emissions, H for historical land cover changes, HYDE is for data by Klein Goldewijk (2001), HGT for Houghton & Hackler (2002); LPJ, Lund–Potsdam–Jena.

Changes in atmospheric $\delta^{13}\text{C}_{\text{CO}_2}$

Both oceanic and terrestrial components of CLIMBER-2 simulate ¹³C cycle (Brovkin *et al.*, 2002). The major effect on atmospheric $\delta^{13}\text{C}_{\text{CO}_2}$ in our simulations should come from the land cover changes and fossil fuel emissions, as both are sources of isotopically lighter CO₂. Dynamics of $\delta^{13}\text{C}$ for fossil fuel emissions are taken from Andres *et al.* (1996). Initial value for atmospheric $\delta^{13}\text{C}_{\text{CO}_2}$ was chosen as -6.2‰ in order to be at the level of ice core data for $\delta^{13}\text{C}_{\text{CO}_2}$ during the 18–19th centuries.

We compare simulated $\delta^{13}\text{C}_{\text{CO}_2}$ in EH and EH-HYDE with Law Dome ice core data (Francey *et al.*, 1999) and measurements for Mauna Loa (Keeling *et al.*, 1989) and Cape Grim (Francey & Allison, 1998) during 1800–2000 (see Fig. 7). Both EH and EH-HYDE simulations broadly agree with the data. The main disagreement is during the 1950–1960s, then the ice core data shows $\delta^{13}\text{C}_{\text{CO}_2}$ by 0.1–0.15‰ higher than simulated. During this period, CO₂ emissions grew sharply, and this led to an abrupt decline of simulated $\delta^{13}\text{C}_{\text{CO}_2}$. This would be a general result for any carbon cycle model. Law Dome data shows this decline but with a delay of one decade. This inconsistency might be caused by inaccuracy in either fossil fuel emission statistics or ice core measurements.

EH-HYDE compares well with ice core during 1850–1950 and Cape Grim data. Over the entire period 1800–2000, EH simulation shows changes in $\delta^{13}\text{C}_{\text{CO}_2}$ by 0.1‰ larger than EH-HYDE. This difference is particularly explained by different temporal evolution of the land cover changes in R&F and HYDE datasets. In both

datasets, the overall changes in land cover are similar, but HYDE has earlier land clearance than R&F. Because the ¹³C cycle is out of equilibrium, earlier release of depleted ¹³C by land in EH-HYDE simulation is buffered by the ocean uptake of ¹³C. This shows that despite similar CO₂ evolution in both simulations, atmospheric $\delta^{13}\text{C}$ is affected by the temporal dynamics of land clearance. EH simulates $\delta^{13}\text{C}_{\text{CO}_2}$ lower by 0.1‰ than Cape Grim data, but is within the range of data variability from Mauna Loa. Therefore the currently available $\delta^{13}\text{C}_{\text{CO}_2}$ datasets are insufficient to evaluate the quality of land cover datasets.

CLIMBER-2-LPJ simulations

Simulation E-LPJ with fossil emission forcing only underestimates the atmospheric CO₂ concentration throughout the 20th century and by 1992, it is lower than observations by 11 ppmv (Fig. 6). In other words, without land-use emissions, the atmospheric CO₂ growth cannot be explained. When considering land cover changes in the EH-LPJ experiment, simulated atmospheric CO₂ follows observations during the first half of the 20th century and deviates after 1950. In 1992, the coupled model overestimates observed CO₂ by 8 ppmv. Overall the effect of land cover changes on atmospheric CO₂, i.e. the difference in atmospheric CO₂ in 1992 between the EH-LPJ and E-LPJ simulations, is 19 ppmv. There are several possible explanations for the overestimated atmospheric CO₂ concentration in the EH-LPJ simulation. Besides a possible too low oceanic

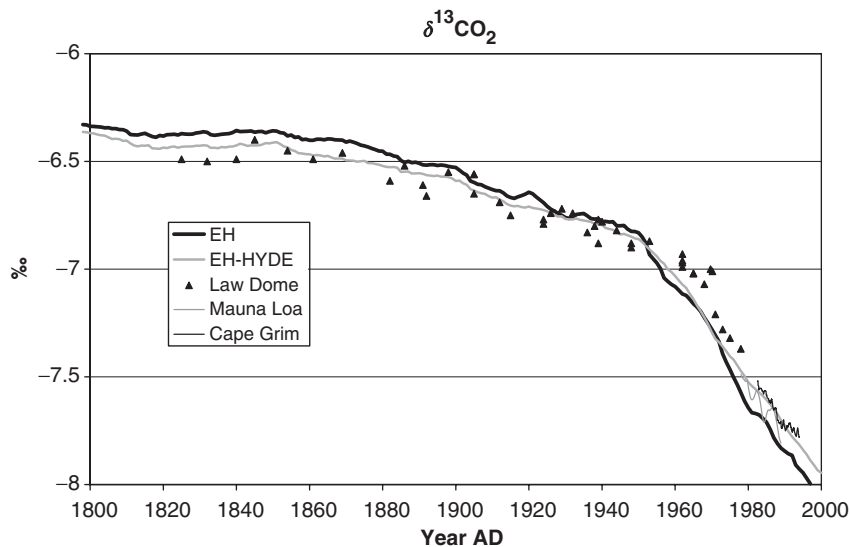


Fig. 7 Atmospheric $\delta^{13}\text{CO}_2$ from the CLIMBER-2 simulations during years 1800–2000 against Low Dome ice core data (Francey *et al.*, 1999), Mauna Loa (Keeling *et al.*, 1989), and Cape Grim observations (Francey & Allison, 1998).

carbon uptake, these include: an overestimation of land cover conversion flux and subsequent fluxes from product pools; an underestimated CO_2 fertilization effect; model oversensitivity to historical climate changes. An overestimation in the land cover conversion flux most likely explains the largest part of the difference. Earlier studies (McGuire *et al.*, 2001) have shown that LPJ tends to overestimate the fluxes associated with land cover change during the 1950s, relative to other biosphere models. Whereas some of the other terrestrial biosphere models assign their vegetation types as input from datasets, LPJ simulates the potential natural vegetation and its corresponding carbon pools. In additional simulations (not shown), we found out that the overestimate in emissions is not due to LPJ simulating an incorrect grassland and savannah distribution (in particular in central Asia) and associated overestimation of biomass. Instead LPJ tends to overpredict carbon storage in the forests and woodlands of European Russia and Eastern Europe. According to the R&F data, large areas of European Russia, Eastern Europe, and Central Asia were converted from natural vegetation into croplands during the 1950s. Thus, overprediction of carbon storage in temperate mixed and boreal forests (Venevsky, 2001) in LPJ leads to the overestimated carbon emissions (see Fig. 8).

Relative role of land cover in atmospheric CO_2 growth

The influence of land cover on atmospheric CO_2 can be measured in different ways. We calculate the difference in CO_2 growth between the simulations with and

without land cover changes, EH and E, respectively, during a time period from t_1 to t_2 :

$$\Delta C_A(E, H, t_1, t_2) - \Delta C_A(E, t_1, t_2), \quad (2)$$

where E and H represent emission and land cover forcings, respectively, and $\Delta C_A(x, t_1, t_2) = C_A(x, t_2) - C_A(x, t_1)$. This is similar to the factor separation technique (Stein & Alpert, 1993) applied for time-series analysis. The point is that the difference between simulations is growing with time and, therefore, is time dependent. We suggest normalizing the difference with regard to observed CO_2 growth:

$$R_1 = (\Delta C_A(E, H, t_1, t_2) - \Delta C_A(E, t_1, t_2)) / \Delta C_A(\text{obs}, t_1, t_2). \quad (3)$$

The indicator R_1 shows the relative role of land cover in atmospheric CO_2 growth measured in percentage of observed CO_2 growth. R_1 indicates the role of land cover forcing relative to fossil fuel forcing evolving through time. Because land and ocean carbon sinks are accounted for in atmospheric CO_2 growth, indicator R_1 does not indicate the individual role of land-use CO_2 emissions in total CO_2 emissions. Note, indicator R_1 is not constrained between 0% and 100%, as it can be higher than 100% in the past as CO_2 growth was very small, or below 0 in the case of afforestation on abandoned cropland. To minimize the effect of climate and CO_2 variability, we apply the indicator for time periods with substantial growth in the observed atmospheric CO_2 . We subdivided years 1850–2000 into time intervals 1850–1900, 1900–1950, and then into decades after 1950 (see Fig. 9). During 1850–1950, all the simulations show a large role of land cover changes:

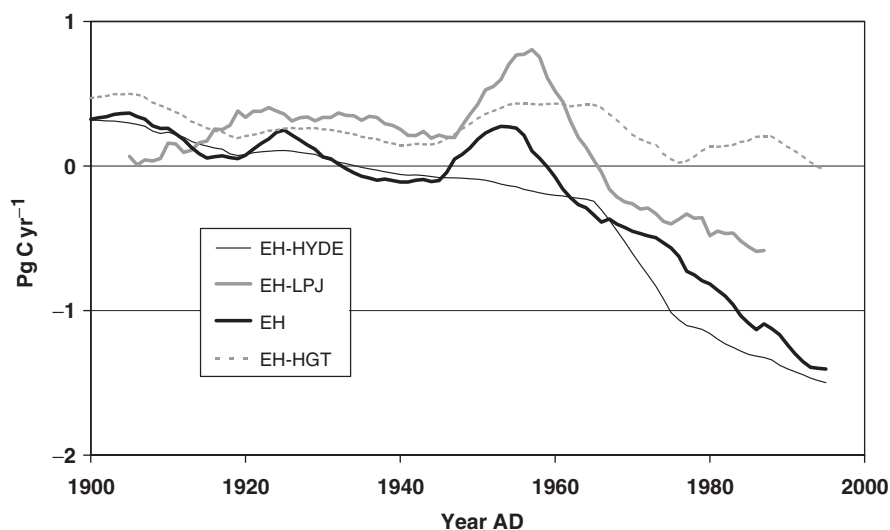


Fig. 8 Simulated net land-atmosphere flux during the 20th century.

about 30–40% for EH and EH-HYDE, 50–60% for EH-HGT and 66% for EH-LPJ, the latter for 1900–1950 as LPJ was initialized with 1900 vegetation cover. During the 1950s, EH, EH-LPJ, and EH-HGT show increase in R_1 while EH-HYDE shows a small decline. In the former simulations, this is caused by an increasing deforestation rate, which is translated into an increase in the net land-atmosphere flux during the 1950–1960s (Fig. 8). A delayed response of EH-LPJ is caused by allocation of a fraction of the converted biomass into the product and litter pools, a process neglected in the EH simulation. The EH-HYDE simulation does not indicate such changes (Fig. 8). This is a clear manifestation of differences between land cover datasets during the 1950s and the 1960s, which is an interesting point for further investigation but is beyond the scope of the given paper.

During decades 1960–1990s, the relative role of land cover changes in atmospheric CO₂ growth was substantially lower than in years 1850–1950 (Fig. 9). The EH and EH-LPJ simulations, which are based on the R&F dataset, show decline in R_1 after a maximum in the 1960–1970s, while EH-HGT has a maximum in the 1990s. This difference may be caused by the timing of tropical deforestation, as has been mentioned by the IPCC (Prentice *et al.*, 2001). EH-HYDE shows a minimum role of land cover change in the 1970s (–1%). This may be due to the coarser spatial resolution of the HYDE dataset with 20 years time interval time slices (1950, 1970, 1990) and increased tropical deforestation during the 1980–1990s as in the HGT dataset. During the latter half of the century, emissions from increasing tropical deforestation are compensated by

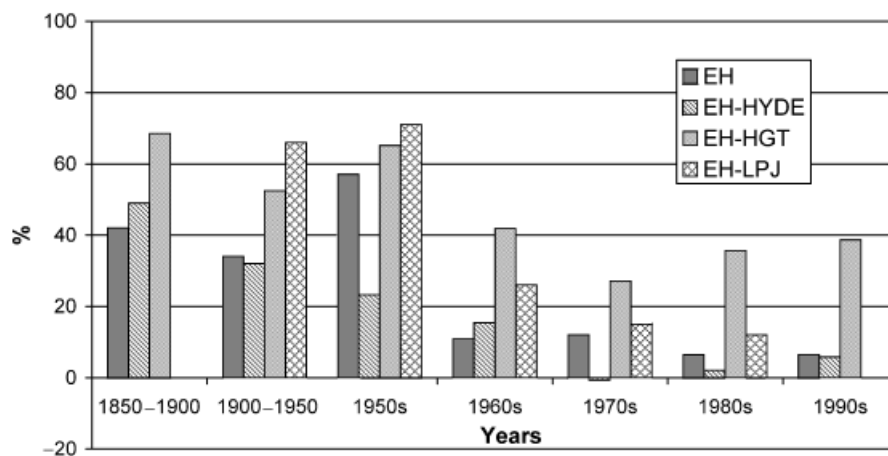


Fig. 9 Relative contribution of land cover changes to atmospheric CO₂ growth, R_1 (%).

forest regrowth on agriculturally abandoned land in temperate ecosystems.

Overall, the values of the indicator R_1 for years 1850–2000 differ among land cover change reconstructions, but the general trend is towards a declining relative role of land cover changes in the atmospheric CO₂ growth (Fig. 9). Presumably, accelerated fossil fuel emissions after the 1950s led to the dominant role of fossil fuel factor in the atmospheric CO₂ growth.

Conclusions

This study presents several novelties: a comparison of biogeophysical and biogeochemical effects of historical land cover changes on climate during the last 150 years; a comparison of several datasets of land cover changes regarding their influence on atmospheric CO₂; and a quantitative analysis of the relative role of land cover changes in atmospheric CO₂ growth.

Anthropogenic land cover changes during the last millennium played an important and complex role in the climatic change. In H_P and H_C simulations with the R&F dataset, biogeophysical mechanisms on a global scale tend to decrease surface air temperature by 0.26 °C due to land cover changes, while biogeochemical mechanisms act to warm the climate by 0.18 °C. The net effect in H simulation is negligible on a global scale, but pronounced over the land in the temperate and high northern latitudes, where a cooling due to an increase in land surface albedo offsets the warming due to land-use CO₂ emissions.

Driven by R&F dataset in the baseline EH simulation, CLIMBER-2 estimates an increase in atmospheric CO₂ in 2000 of 24 ppmv higher than in simulation E without land cover forcing. This increase is equally distributed during the periods prior to 1850, 1850–1940, and thereafter. Averaged over 50-year periods, absolute role of land cover changes in atmospheric CO₂ growth (ppmv yr⁻¹) increases with time. To quantify the relative role of land cover changes, we introduce an indicator R_1 , which shows the effect of land cover on atmospheric CO₂ measured in percentage of observed CO₂ growth. In the EH simulation, R_1 averaged over the last millennium is 26%. It declined from 88% between 1000 and 1850 to 6% during the 1990s.

Data and model are subject to uncertainty. Uncertainty in reconstructing land-use history was tested by applying two datasets, HYDE and HGT. The experiments reveal that during the last millennium, land cover changes led to an increase in atmospheric CO₂ by 22–43 ppmv corresponding to 25–49% of observed CO₂ growth. This contribution declines from $36 \pm 60\%$ during 1850–1960 to $4 \pm 35\%$ during 1960–2000. In simulations of coupled CLIMBER-2 and advanced

vegetation model, LPJ, land cover contribution to the atmospheric CO₂ growth decreases from 68% during 1900–1960 to 12% in the 1980s. In all simulations with CO₂ emission forcing, the constant atmospheric CO₂ during the 1940s inferred from the Law Dome ice core was not reproduced.

The declining relative role of land cover is not new, but here we present the first attempt to quantify this role directly in terms of atmospheric CO₂ forcing, not emissions. Additionally, we used several geographically explicit land-use datasets (R&F and HYDE). This is a clear advance on carbon cycle studies using box models, e.g. by Keeling *et al.* (1989), which do not account for numerous mechanisms in the climate–biogeochemistry system, limiting their ability to quantify land cover emissions.

In EH and EH-HYDE simulations, we calculated the dynamics of atmospheric $\delta^{13}\text{CO}_2$. Over the entire period from 1800–2000, EH-HYDE compares well with ice core during 1850–1950 and Cape Grim data, while EH simulation shows changes in $\delta^{13}\text{CO}_2$, 0.1‰ larger than EH-HYDE. Despite similar CO₂ evolution in both simulations, atmospheric $\delta^{13}\text{CO}_2$ is affected by the temporal dynamics of land clearance: EH-HYDE has earlier land clearance than R&F. However, $\delta^{13}\text{CO}_2$ data from EH are within the range of data variability from Mauna Loa. Therefore, given the uncertainty among ¹³CO₂ measurements, the $\delta^{13}\text{CO}_2$ data cannot be used to evaluate the quality of the simulations (and land cover datasets).

In EH-HGT simulation, atmospheric CO₂ growth during the second part of the 20th century is 74 ppmv, 16 ppmv higher than observed. Jones *et al.* (2003) showed that coupled climate–carbon cycle Hadley Centre model, driven by IS92a scenario of fossil fuel and land-use emissions (HGT till the 1990s), overestimates atmospheric CO₂ concentration in 2000 by 15 ppmv. However, the model closely follows observed CO₂ trend if they account for 30% reduction in land-use emissions. Their run and our EH-HGT simulation indicate that bookkeeping estimates of land-use emissions might be too high. Nonetheless, one cannot exclude the possibility that models underestimate uptake of carbon by natural vegetation since simulations do not account for some processes, for example the fertilization effect of anthropogenic nitrogen depositions (Prentice *et al.*, 2001).

Atmospheric CO₂ changes of ca. 90 ppmv during historical period are small in comparison with expected changes of 300–400 ppmv during the 21st century (Prentice *et al.*, 2001). If fossil fuel emissions continue to grow in the future, one can expect a further decline in the relative role of land cover changes during the 21st century. However, in absolute terms, emissions due to

future changes in land cover are likely to be large but highly uncertain (House *et al.*, 2002). Moreover, recent studies indicate that future uncertainty in tropical land-use projections are far more important than the choice of GCM climate scenario for the carbon cycle in the tropics (Cramer *et al.*, 2004).

Reproducing historical changes in atmospheric CO₂ is one of the few tests available, before application of coupled climate–carbon cycle models for the CO₂ emission and land cover scenarios. A good quality of reconstruction of historical land cover changes is important. Our simulations confirm that without accounting for the historical land cover changes, the observed atmosphere CO₂ growth cannot be explained.

Acknowledgements

The authors thank Kees Klein Goldewijk for providing us with natural vegetation data from the HYDE dataset. We also thank Joanna House, Colin Prentice, Richard Betts and two anonymous reviewers for thoughtful comments on earlier drafts of this paper.

References

- Andres RJ, Marland G, Bischof S (1996) *Global and latitudinal estimates of $\delta^{13}\text{C}$ from fossil-fuel consumption and cement manufacture*. DB1013, CDIAC, ORNL, Oak Ridge.
- Avisar R, Silva Dias PL, Silva Dias MAF *et al.* (2002) The large-scale biosphere–atmosphere experiment in Amazonia (LBA): insights and future research needs. *Journal of Geophysical Research*, **107**, 8086, doi:10.1029/2002JD002704.
- Bauer E, Claussen M, Brovkin V (2003) Assessing climate forcings of the Earth system for the past millennium. *Geophysical Research Letters*, **30**, 1276, doi:10.1029/2002GL016639.
- Bertrand C, Loutre MF, Crucifix M *et al.* (2002) Climate of the last millennium: a sensitivity study. *Tellus A*, **54**, 221–244.
- Betts RA (2001) Biogeophysical impacts of land use on present-day climate: near-surface temperature and radiative forcing. *Atmospheric Science Letters*, **2**, 39–51.
- Bonan GB, Pollard D, Thompson SL (1992) Effects of boreal forest vegetation on global climate. *Nature*, **359**, 716–718.
- Bopp L, Le Quéré C, Heimann M *et al.* (2002) Climate-induced oceanic oxygen fluxes: implications for the contemporary carbon budget. *Global Biogeochemical Cycles*, **16** doi:10.1029/2001GB001445.
- Brovkin V, Bendtsen J, Claussen M *et al.* (2002) Carbon cycle, vegetation and climate dynamics in the Holocene: experiments with the CLIMBER-2 model. *Global Biogeochemical Cycles*, **16**, 1139, doi:10.1029/2001GB001662.
- Brovkin V, Ganopolski A, Claussen M *et al.* (1999) Modelling climate response to historical land cover change. *Global Ecology and Biogeography*, **8**, 509–517.
- Brovkin V, Levis S, Loutre MF *et al.* (2003) Stability analysis of the climate–vegetation system in the northern high latitudes. *Climatic Change*, **57**, 119–138.
- Chase TN, Pielke RA, Kittel TGF *et al.* (2000) Simulated impacts of historical land cover changes on global climate in northern winter. *Climate Dynamics*, **16**, 93–105.
- Claussen M, Brovkin V, Ganopolski A *et al.* (1999) A new model for climate system analysis: outline of the model and application to palaeoclimate simulations. *Environmental Modelling and Assessment*, **4**, 209–216.
- Claussen M, Brovkin V, Ganopolski A (2001) Biogeophysical versus biogeochemical feedbacks of large-scale land cover change. *Geophysical Research Letters*, **28**, 1011–1014.
- Claussen M, Mysak LA, Weaver AJ *et al.* (2002) Earth system models of intermediate complexity: closing the gap in the spectrum of climate system models. *Climate Dynamics*, **18**, 579–586.
- Cox P, Betts R, Jones C *et al.* (2000) Acceleration of global warming due to carbon-cycle feedbacks in a coupled climate model. *Nature*, **408**, 184–187.
- Cramer W, Bondeau A, Lucht W *et al.* (2004) Tropical forests and the global carbon cycle: simulations for the 20th century reconstruction and future scenarios. *Philosophical Transactions of the Royal Society, Series B – Biological Series*, **359**, 331–343 doi: 10.1098/rstb.2003.1428.
- Crowley TJ (2000) Causes of climate change over the past 1000 years. *Science*, **289**, 270–277.
- De Fries RS, Bounoua L, Collatz GJ (2002) Human modification of the landscape and surface climate in the next fifty years. *Global Change Biology*, **8**, 438–458.
- Etheridge DM, Steele LP, Langenfelds RL *et al.* (1996) Natural and anthropogenic changes in atmospheric CO₂ over the last 1000 years from air in Antarctic ice and firn. *Journal of Geophysical Research*, **101**, 4115–4128.
- Francey RJ, Allison CE (1998) *In situ $\delta^{13}\text{C}$ CO₂ from Cape Grim, Tasmania, Australia: 1982–1993*. In: *Trends*. CDIAC, ORNL, Oak Ridge.
- Francey RJ, Allison CE, Etheridge DM *et al.* (1999) A 1000 year high precision record of $\delta^{13}\text{C}$ in atmospheric CO₂. *Tellus Series B*, **51**, 170–193.
- Forest CE, Stone PH, Sokolov AP *et al.* (2002) Quantifying uncertainties in climate system properties with the use of recent climate observations. *Science*, **295**, 113–117.
- Friedlingstein P, Bopp L, Ciais P *et al.* (2001) Positive feedback between future climate change and the carbon cycle. *Geophysical Research Letters*, **28**, 1543–1546.
- Ganopolski A, Petoukhov V, Rahmstorf S *et al.* (2001) CLIMBER-2: a climate system model of intermediate complexity. Part II: validation and sensitivity tests. *Climate Dynamics*, **17**, 735–751.
- Gerber S, Joos F, Brügger P *et al.* (2003) Constraining temperature variations over the last millennium by comparing simulated and observed atmospheric CO₂. *Climate Dynamics*, **20**, 281–299.
- Henderson-Sellers A, Dickinson RE, Durbidge TB *et al.* (1993) Tropical deforestation – modeling local-scale to regional-scale climate change. *Journal of Geophysical Research*, **98**, 7289–7315.
- Houghton RA, Hackler JL (2002) Carbon flux to the atmosphere from land-use changes. In: *Trends*. CDIAC, ORNL, Oak Ridge.
- Houghton RA, Hobbie JE, Melillo JM *et al.* (1982) Changes in the carbon content of terrestrial biota and soils between 1860 and 1980: a net release of CO₂ to the atmosphere. *Ecological Monographs*, **53**, 235–262.

- House JI, Prentice IC, LeQuéré C (2002) Maximum impacts of future reforestation or deforestation on atmospheric CO₂. *Global Change Biology*, **8**, 1047–1052.
- Jones CD, Cox PM, Essery RLH *et al.* (2003) Strong carbon cycle feedbacks in a climate model with interactive CO₂ and sulphate aerosols. *Geophysical Research Letters*, **30**, 1479, doi:10.1029/2003GL016867.
- Jones PD, Parker DE, Osborn TJ *et al.* (2001) Global and hemispheric temperature anomalies – land and marine instrumental records. In: *Trends*. CDIAC, ORNL, Oak Ridge.
- Joos F, Meyer R, Bruno M *et al.* (1999) The variability in the carbon sinks as reconstructed for the last 1000 years. *Geophysical Research Letters*, **26**, 1437–1440.
- Keeling CD, Bacastow RB, Carter AF *et al.* (1989) A three-dimensional model of atmospheric CO₂ transport based on observed winds: analysis of observational data. *AGU Geophysical Monograph*, **55**, 165–236.
- Keeling CD, Whorf TP (2002) Atmospheric CO₂ records from sites in the SIO air sampling network. In: *Trends*. CDIAC, ORNL, Oak Ridge.
- Klein Goldewijk K (2001) Estimating global land use change over the past 300 years: the HYDE database. *Global Biogeochemical Cycles*, **15**, 417–433.
- Leemans R, Eickhout B, Strengers B *et al.* (2002) The consequences of uncertainties in land use, climate and vegetation responses on the terrestrial carbon. *Science in China (Series C)*, **45** (Suppl.), 126–145.
- Matthews HD, Weaver AJ, Eby M *et al.* (2003) Radiative forcing of climate by historical land cover change. *Geophysical Research Letters*, **30**, 1055, doi:10.1029/2002GL016098.
- Marland G, Boden TA, Andres RJ (2002) Global, regional, and national fossil fuel CO₂ emissions. In: *Trends*. CDIAC, ORNL, Oak Ridge.
- McGuire AD, Sitch S, Clein JS *et al.* (2001) Carbon balance of the terrestrial biosphere in the twentieth century: analyses of CO₂, climate and land use effects with four process-based ecosystem models. *Global Biogeochemical Cycles*, **15**, 183–206.
- New M, Hulme M, Jones PD (1999) Representing twentieth century space-time climate variability. Part I: development of a 1961–90 mean monthly terrestrial climatology. *Journal of Climate*, **12**, 829–856.
- New M, Hulme M, Jones P (2000) Representing twentieth-century space-time climate variability. Part II: development of 1901–96 monthly grids of terrestrial surface climate. *Journal of Climate*, **13**, 2217–2238.
- Petoukhov V, Ganopolski A, Brovkin V *et al.* (2000) CLIMBER-2: a climate system model of intermediate complexity. Part I: model description and performance for present climate. *Climate Dynamics*, **16**, 1–17.
- Prentice IC, Farquhar GD, Fasham MJR *et al.* (2001) The carbon cycle and atmospheric carbon dioxide. In: *Climate Change 2001: The Scientific Basis* (eds Houghton JT), Cambridge University Press, New York.
- Plattner GK, Joos F, Stocker TF (2002) Revision of the global carbon budget due to changing air-sea oxygen fluxes. *Global Biogeochemical Cycles*, **16** doi:10.1029/2001GB001746.
- Ramankutty N, Foley JA (1999) Estimating historical changes in global land cover: croplands from 1700 to 1992. *Global Biogeochemical Cycles*, **13**, 997–1027.
- Sitch S, Smith B, Prentice IC *et al.* (2003) Evaluation of ecosystem dynamics, plant geography and terrestrial carbon cycling in the LPJ dynamic global vegetation model. *Global Change Biology*, **9**, 161–185.
- Stein U, Alpert P (1993) Factor separation in numerical simulations. *Journal of the Atmospheric Sciences*, **50**, 2107–2115.
- Thonicke K, Venevsky S, Sitch S *et al.* (2001) The role of fire disturbance for global vegetation dynamics: coupling fire into a Dynamic Global Vegetation Model. *Global Ecology and Biogeography*, **10**, 661–677.
- Venevsky S (2001) *Broad-scale vegetation dynamics in north-eastern Eurasia – observations and simulations*. PhD thesis, Universität für Bodenkultur Wien.
- Vitousek PM, Mooney HA, Lubchenco J *et al.* (1997) Human domination of earth's ecosystems. *Science*, **277**, 494–499.
- Wigley TML, Raper SCB (1992) Implications for climate and sea level of revised IPCC emissions scenarios. *Nature*, **357**, 293–300.